

Cross section of ILRS satellites

by

David A. Arnold

1. Introduction

The cross section of the satellites tracked by ILRS has been computed using whatever information is available on the design of the arrays and the specifications of the cube corners. The cross section is not constant for any array. It is a function of incidence angle, velocity aberration, wavelength, and polarization if the cube corners are uncoated. The cross section is given by the intensity of the diffraction pattern of the array at the position of the receiver in the far field as determined by the velocity aberration. This report uses diffraction theory to calculate cross section matrices for the arrays at various incidence angles for wavelength 532 nanometers. The velocity aberration limits depend on the altitude of the satellite. The average cross section within the velocity aberration limits is computed at each incidence angle on the array. The average over all incidence angles is also computed and tabulated.

2. Cross section table.

Table 1 lists the current cross section for each satellite on the ILRS webpage and the revised cross section computed using diffraction theory. The minimum and maximum cross section as a function of velocity aberration and incidence angle are also listed for the satellites where there is enough information to do a diffraction calculation.

THEORETICAL CROSS SECTION (Million sq m)					
SATELLITE	ALTITUDE	CURRENT	REVISED		
			Minimum	Average	Maximum
Starlette	950	0.65	1.00	1.80	2.5
Lageos	6000	7.00	9.00	15.00	23.0
Etalon	19000	60.00	-	55.00	-
Topex	1300	2.00	6.00	33.00	83.0
BeaconC	940	3.60	0.00	13.00	35.0
Ajisai	1400	12.00	-	23.00	-
Gfo-1	800	2.00	.07	.50	1.1
Stella	950	0.65	1.00	1.80	2.5
Jason	1300	0.30	.20	.80	1.7
GPS	20000	40.00	-	19.00	-
Champ	500	1.80	.05	1.00	3.4
Westpac	835	0.03	0.00	.04	.4
ERS	800	0.30	.20	.85	1.6
Glomass396	20000	360.00	-	240.00	-
Glomass132	20000		-	80.00	-
Envisat	800	0.30	.20	.85	1.6
LRE	25000	1.25	-	2.00	-
SUNSAT	600	0.20	.04	.40	1.4

Table 1. Current and revised cross section for the ILRS satellites.

3. Diffraction model.

The diffraction calculations have been done using the theory given in SAO Special Report 382, "Method of Calculating Retroreflector Array Transfer Functions", David A. Arnold. The equations model coated or uncoated retroreflectors with a dihedral angle offset. The model does not include any manufacturing imperfections such as roughness or surface curvature. Manufacturing imperfections can result in a loss of cross section in the actual cube corners. These losses are probably a factor of 2 or more. Therefore the theoretical calculations should be considered as an upper limit to the actual cross section. There is no data on the actual "in-orbit" cross section in absolute units although relative measurements between some satellites have been done.

The cube corners on the Japanese satellites are in the shape of a triangle with the corners cut off. There is no model for the reflectivity of this design of cube corner. The Russian satellites are not manufactured to a particular specification. Therefore it is not possible to do an accurate theoretical calculation of the cross section. For satellites where no information is available on the dihedral angle offset, an angle optimized for the particular velocity aberration has been used. If the actual dihedral angle is not optimized, the cross section will probably be lower.

The Japanese satellites are spherical and use uncoated cube corners. Since the LAGEOS satellite is also spherical and uses uncoated cube corners, the cross section of the Japanese satellites is estimated by scaling the cross section of LAGEOS by the reflecting area.

4. Sample diffraction patterns.

Diffraction patterns of various satellites are shown in the report "Retroreflector Array Transfer Functions" available on the web at <http://nercslr.nmt.ac.uk/sig/signature.html> in PDF and WORD format (Reference 1). Some sample diffraction patterns for LAGEOS from that report are shown in Figure 1 for linear and circular polarization.

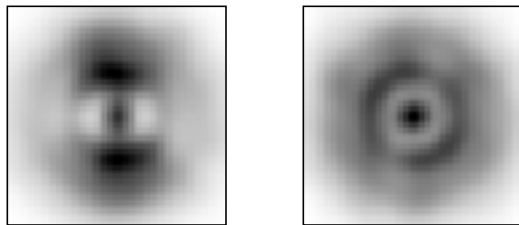


Figure 1. Cross section of LAGEOS for linear polarization (left) and circular polarization (right) at one orientation of the satellite. The axes are -50 to +50 microradians.

The diffraction pattern for linear polarization has a dumbbell shape with the axis of the dumbbell aligned with the polarization vector of the incident laser beam. The diffraction pattern for circular polarization has a more circular shape. The pattern for circular polarization is not perfectly circular because there are a limited number of cube corners that are active at a particular orientation of the satellite. The intensity of the diffraction pattern at the position of the receiver is the cross section of the satellite.

Figure 2 shows some sample diffraction patterns for TOPEX from Reference 1.

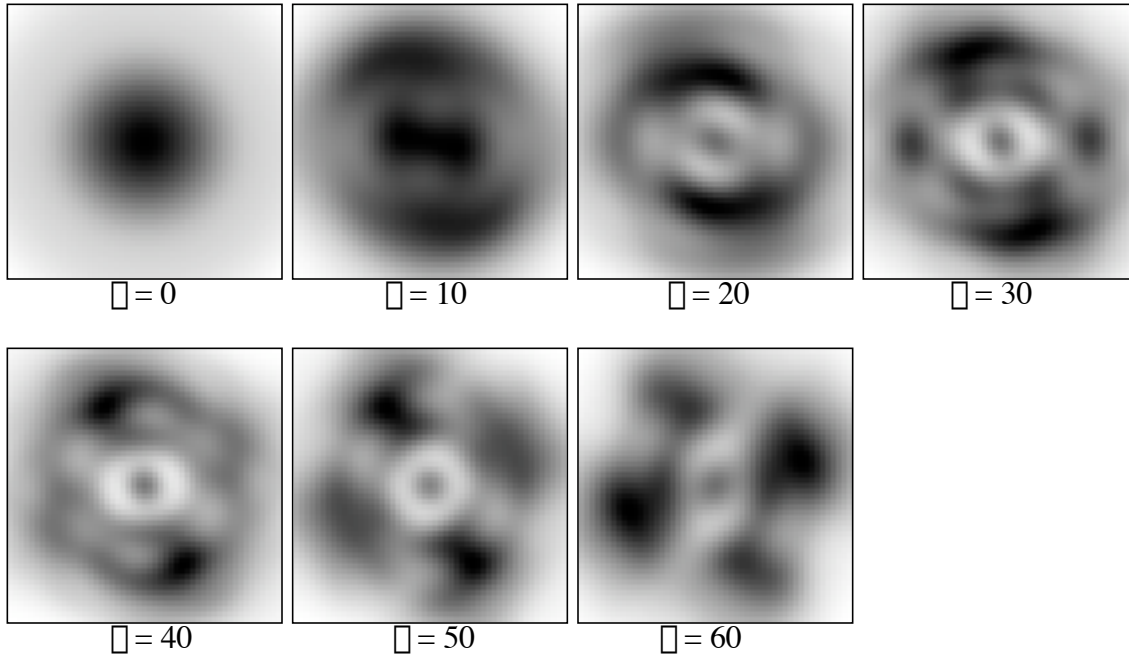


Figure 2. Diffraction patterns of the TOPEX retroreflector array for various incidence angles on the array.

5. Variation of the cross section with incidence angle.

A. TOPEX

As can be seen from figure 2 the cross section varies with incidence angle as well as with the position of the receiver in the far field pattern as determined by the magnitude and direction of the velocity aberration. Table 2 shows a summary of the cross section for TOPEX vs incidence angle on the array.

Cross section of TOPEX (million sq m)

Incidence Angle	Minimum	Average	Maximum	Active area
0	15	20	32	31
10	15	29	40	34
20	16	37	62	37
30	19	44	71	40
40	12	45	83	40
50	12	35	62	32
60	6	22	38	21

Table 2. Cross section statistics for TOPEX. The first column is the incidence angle in degrees, the second the minimum cross section, the third the average cross section between 25 and 50 microradians velocity aberration, the fourth the maximum cross section, and the fifth the total reflecting area in equivalent number of cube corners at normal incidence.

The average of the numbers in the third column is 33 million sq meters. The lowest cross section is 6 million at the bottom of column 2 and the highest cross section is 83 million in column 4 for 40 degrees incidence angle. This is the data that was used to generate the values in Table 1 for TOPEX.

B. SUNSAT

The Sunsat array has a ring of 8 cube corners tilted at 50 degrees with respect to the symmetry axis. There is no pole cube facing the earth such as on the ERS, JASON, GFO, and other similar satellites. The 9 cube arrays on these other satellites form an approximate hemisphere so that the cross section does not vary much with incidence angle. For the Sunsat array, the cross section at normal incidence on the array is very low because all the cube corners are being viewed at a 50 degree incidence angle. This is not far from the cutoff angle of about 57 degrees. The fact that the cross section is very low for normal incidence is not a problem because this only occurs at zenith where the range is shortest. In fact the absence of the pole cube can be an advantage in avoiding a large dynamic range in the signal. However, using a constant cross section in predicting signal strength would result in large errors since there is such a large variation in cross section. Figure 3 shows the variation of the cross section for Sunsat with incidence angle on the array.

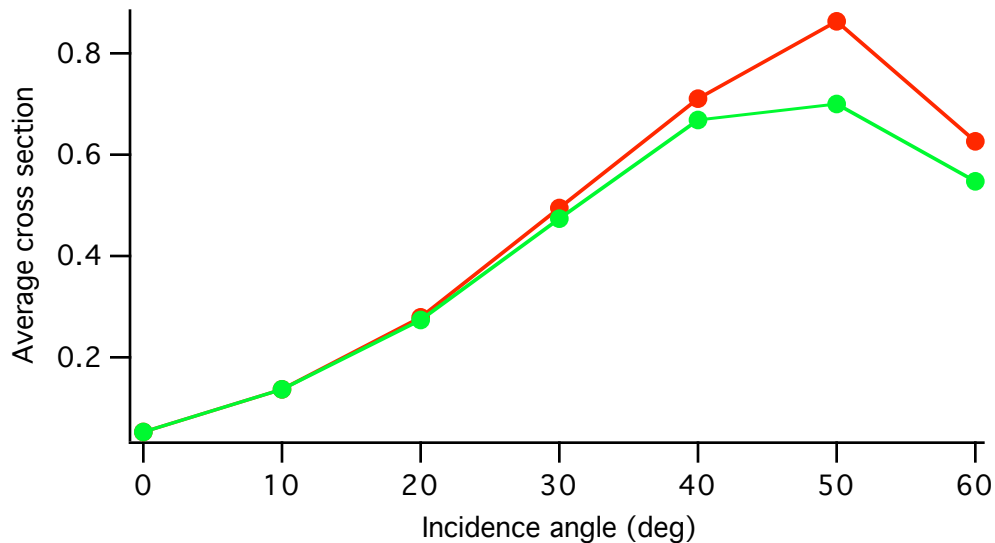


Figure 3. Cross section of Sunsat vs incidence angle (deg) on the array. The top curve (red) is for Theta = 0 deg and the bottom curve (green) is for Theta = 22.5 deg which is between the first two cube corners in the ring.

C. BEACON

Figure 4 shows a diagram of the BeaconC array. There is one panel at the top and 8 panels tilted at a 54 degree angle. The satellite is magnetically stabilized. Figure 5 shows the cross section vs incidence angle on the array. The green curve is between two panels so the cross section is lower. The cutoff angle is about 105 degrees. The cross section is reasonably constant up to about 70 degrees, but using a constant cross section would give a large error near the cutoff angle.

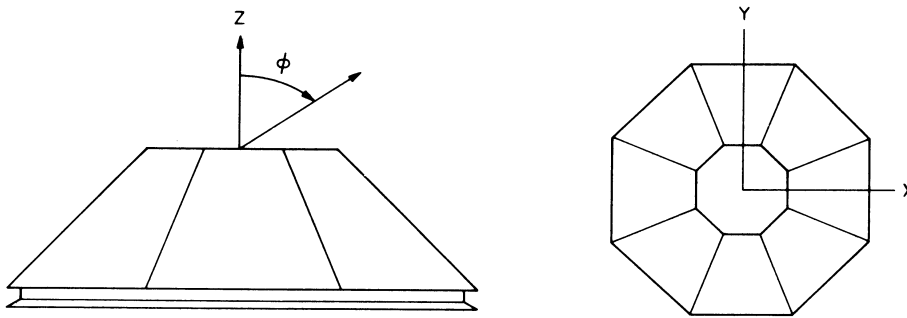


Figure 4. Diagram of the Beacon retroreflector array.

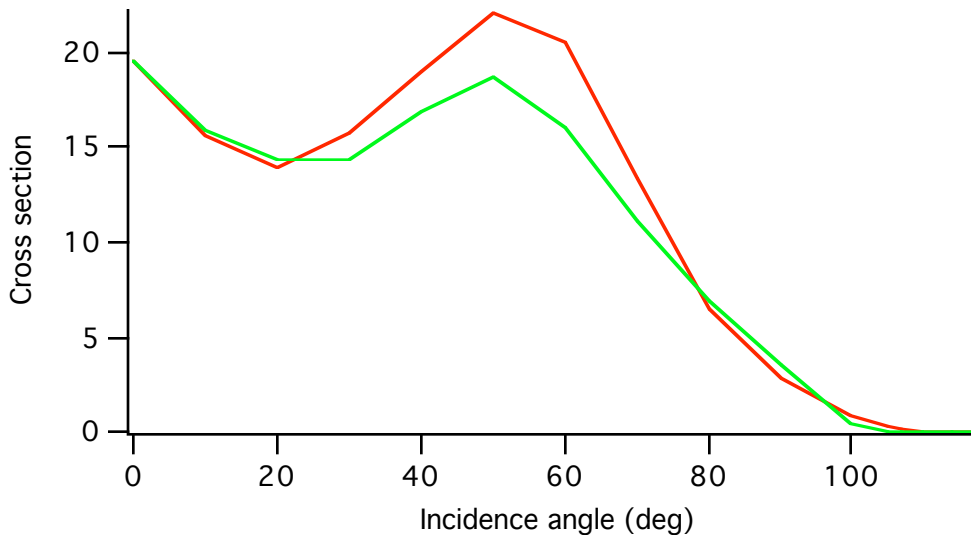


Figure 5. Cross section of the BeaconC array vs incidence angle. The top curve (red) is for Theta = 0 deg and the bottom curve (green) is for Theta = 22.5 deg.

D. CHAMP, GRACE

The cross section of CHAMP is fully documented in References 2 and 3. The array has 4 cubes on a 45 degree pyramid. Table 3 below summarizes the variations with incidence angle on a cube corner using the data in Reference 2. The cross section near zenith (about 40 deg incidence angle on a cube) is fairly low. However, the range is short so the design reduces the dynamic range of the signal strength. Using the cross section vs incidence angle on a cube would help to reduce the error in the predicted signal strength.

Incidence Angle	Flux			Cross Sec.		
	Minimum	Average	Maximum	Minimum	Average	Maximum
0	.0281	.0281	.0281	3.03	3.03	3.03
10	.0172	.0217	.0312	1.85	2.34	3.37
20	.00623	.0102	.0183	.67	1.10	1.98
30	.00216	.00356	.00680	.23	.38	.73
40	.00044	.00081	.00167	.047	.087	.180

Table 3. Cross section of CHAMP, and GRACE vs incidence angle on a cube corner. The cross section in million sq m is the flux times 108.

D. WESTPAC.

The WESTPAC array is designed so that only one cube corner is active at a time. This is done by recessing the cubes so that the cutoff angle is 13 degrees. This creates dead spaces where there is no signal between the cube corners. Table 4 shows the cross section as a function of incidence angle on a cube corner. The cross section is reasonably constant in the range 0 to 9 degrees and then drops off sharply.

Angle	Average	Max
0	.043	.121
1	.043	.202
2	.045	.284
3	.049	.348
4	.054	.380
5	.060	.373
6	.064	.332
7	.062	.266
8	.054	.188
9	.040	.114
10	.024	.055
11	.010	.018
12	.002	.002
13	.000	.000

Table 4. Average and maximum cross section as a function of incidence angle (deg).

E. Spherical, hemispherical, and planar arrays.

For spherical satellites such as LAGEOS, AJISAI, LRE, and ETALON, STARLETTE, and STELLA the cross section will vary some with velocity aberration but the average cross section is nearly independent of incidence angle.

Arrays that are approximately hemispherical such as ERS, ENVISAT, JASON, and GFO have cross section that do not vary much with incidence angle the same as the spherical satellites.

The high altitude satellites such as GLONASS, GPS have planar arrays. The cross section will vary some with incidence angle but the cross section is reasonably constant.

6. Cross section matrices.

The most accurate method of predicting the signal strength is to use the full cross section matrix to calculate the cross section as a function of the magnitude and direction of the velocity aberration. This procedure was used for the range correction on TOPEX. Because of the large size of the array the variations with velocity aberration were a few centimeters. Since signal strength predictions do not require the same accuracy as range corrections there is probably no need to do this for the cross section.

7. Summary.

The cross section of a retroreflector array may be relatively constant for some satellites and may have large variations for others. The cross section vs incidence angle or the full cross section matrix can be used to obtain more accurate signal strength predictions for satellites where there are large variations in the cross section.

8. References.

1. "Retroreflector array transfer functions", David A. Arnold, Proceedings of the 13th International Workshop on Laser Ranging, October, 2002, Washington, DC.
2. Calculation of the Far field energy distribution of the CHAMP satellite retroreflector, Final report, prepared by: Jakob Neubert, IOF Jena, 1997, Fraunhofer Institut, Angewandte Optik und Feinmechanik.
3. "Investigation of the Effects of Aberration and Diffraction on the Performance of the Laser Reflector for the CHAMP Satellite", prepared by Reinhart Neubert
GeoForschungsZentrum Potsdam, Dev.1: Kinematics and Dynamics of the Earth
Telegrafenberg A17, D-14473 Potsdam, Germany
Tel.: (49)-331-288-1153, Fax.: (49)-331-288-1111, e-mail: neub@gfz-potsdam.de
4. Detailed data and reports for each satellite are available from the author or the Signal Processing Working Group (SPWG), Graham Appleby.